Biointerface Research in Applied Chemistry
Platinum Open Access Journal (ISSN: 2069-5837)

Article
Volume 11, Issue 6, 2021, 13779 - 13789
https://doi.org/10.33263/BRIAC116.1377913789

A One-Pot Multicomponent Catalytic Synthesis of New 1*H*-Pyrazole-1-Carbothioamide Derivatives with Molecular Docking Studies as COX-2 Inhibitors

Tamer K. Khatab [1], Ez-el-din M. Kandil [2], Doaa E. Elsefy [2], Ahmed El-Mekabaty [2,*]

1 Organometallic-Organometalloid Chemistry Department, Chemical Industries Research Division, National Research Centre, 33 El-Behouth St., Dokki, 12622, Cairo, Egypt
2 Chemistry Department, Faculty of Science, Mansoura University, El-Gomhoria Street, 35516 Mansoura, Egypt
* Correspondence: elmekabaty@mans.edu.eg (A.E-M.);

Scopus Author ID 55206382000
Received: 15.01.2021; Revised: 14.02.2021; Accepted: 18.02.2021; Published: 1.03.2021

Abstract: A simple and efficient catalytic synthesis of new 1*H*-pyrazole-1-carbothioamide derivatives through a one-pot reaction of hydrazine hydrate, arylidene malononitrile and isothiocyanates in the presence of HAp/$ZnCl_2$ nano-flakes at 60-70°C has been described. The protocol's main advantages include high yields of products, a wide range of substrates, simple procedure, and short reaction time. Molecular docking studies of the designed compounds were accomplished as COX-2 inhibitors and showed that compounds 3d, 3e, 3h, and 3n give promising results compared with celecoxib as a reference drug.

Keywords: pyrazole; carbothioamide; arylidene malononitrile; anti-inflammatory; nano catalyst.

1. Introduction

In recent decades, inflammation treatment is considered one of the great challenges and has received significant attention [1, 2]. There are two ways for this, the first is through the use of steroidal anti-inflammatory agents, but they have serious side effects and need to withdraw gradually from the human body [3]. The second one uses non-steroidal anti-inflammatory drugs that block pro-inflammatory prostaglandins' production by inhibiting cyclooxygenase (COX), but has side effects like gastritis, ulcer, bleeding and renal impairment [4-6]. The study of the cyclooxygenase enzyme (COX) and its isozymes was a breakthrough in knowing the inflammation process [7]. At least two isoforms of COX are known, COX-1 and COX-2. Since COX-2 is considered responsible for the formation of inflammatory prostaglandins [8], selective COX-2 inhibitors are among the most commonly used drugs. However, many have undesirable side effects [9]. So the search for novel selective COX-2 inhibitors is urgently required. On the other hand, pyrazole derivatives are well established as an important class of heterocyclic compounds that have significant biological activities [10-12]. They are widely employed as potent anti-inflammatory agents and, in many cases, have good selectivity for COX-2 inhibition [13-15]. Some noteworthy examples of marketed selective COX-2 inhibitor drugs containing pyrazole as a central core are shown in Figure 1. Numerous catalytic syntheses of *N*-substituted pyrazole derivatives have been presented over the last decade. However, some often suffer from high coast, long reaction time, low availability, the narrow application scope of substrates, and drastic reaction conditions [16-21]. To the best of our knowledge, there have

been rare methods for the synthesis of 1*H*-pyrazole-1-carbothioamide derivatives. We have recently published the synthesis of hydroxyapatite/$ZnCl_2$ nano-flakes and used them as a highly effective, cheap, reusable, and stable solid catalyst for the synthesis of 2-aryl benzothiazoles [22]. As part of our ongoing research on the development of organic catalytic synthesis [23-26], we have described a simple and efficient one-pot procedure for synthesizing new 1*H*-pyrazole-1-carbothioamide derivatives using HAp/$ZnCl_2$ nano-flakes and study their biological importance as COX-2 inhibitors.

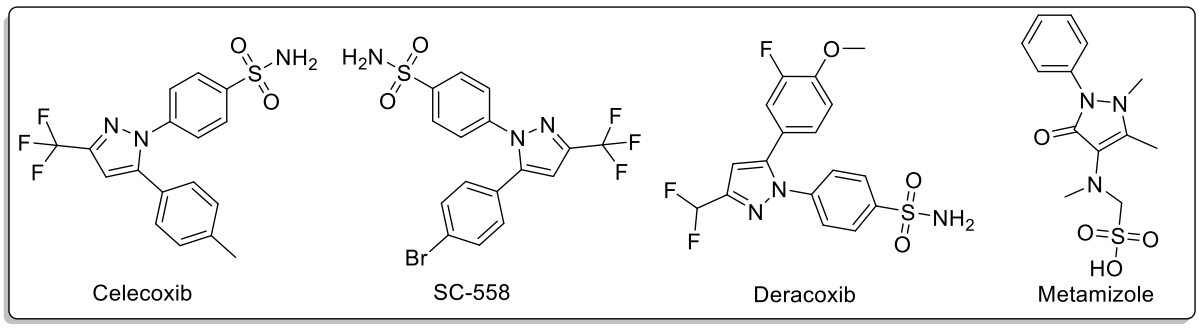

Figure 1. Chemical structure of some pyrazole-containing anti-inflammatory drugs

2. Materials and Methods

Melting points were determined on an electrothermal Gallenkamp apparatus (Germany) and are uncorrected. The IR spectra were measured on a Mattson 5000 FTIR Spectrometer (USA) in potassium bromide discs. The ^{1}H-NMR and ^{13}C-NMR spectra were measured on a Bruker Avance III spectrometer (Germany) at 400 and 100 MHz. The mass spectra were recorded on Kratos MS (Kratos Analytical Instrument, Ramsey, NJ) apparatus (USA) and the ionizing voltage was 70 eV. Elemental analyses have been achieved by the Micro-analytical unit of the Faculty of Science, Cairo University, Egypt. All reactions in the present consideration have been followed by TLC (silica gel, aluminum sheets 60 F254, Merck).

General procedure for one-pot catalytic synthesis of new 1*H*-pyrazole-1-carbothioamide derivatives 3a-n: A mixture of hydrazine hydrate (1 mmol), arylidene malononitrile (1 mmol), isothiocyanates (1 mmol), and a catalytic amount of HAp/$ZnCl_2$ (10 wt%) was stirred at 60-70°C for an appropriate time (Table 1). After completing the reaction (monitored by TLC), the pure organic products were extracted by chloroform and recrystallized from ethanol.

5-Amino-4-cyano-*N*-cyclohexyl-3-phenyl-1*H*-pyrazole-1-carbothioamide (3a): brown crystals; IR (KBr, cm^{-1}) ν_{max}: 3344, 3290 (NH_2), 3150 (NH), 2928, 2853 (C-H, aliphatic), 2211 (CN), 1631 (C=N), 1529 (C=C), 1159 (C=S); ^{1}H-NMR (DMSO) δ (ppm): 11.45 (s, 1H, NH), 8.08 (s, 2H, NH_2), 7.95-7.35 (m, 5H, Ar-H), 4.44-1.23 (m, 11H, cyclohexyl-H); ^{13}C-NMR (DMSO) δ (ppm): 173.85 (C=S), 169.73, 160.12, 133.28, 129.50, 128.71, 127.15, 114.00 (CN), 111.77 (Ar-C), 57.18, 32.51, 26.88, 26.66 (cyclohexyl-C); MS (*m/z*, %): 325 (M^+, 67). Anal. Calcd for $C_{17}H_{19}N_5S$ (325.43): C, 62.74; H, 5.89; N, 21.52; S, 9.85%. Found: C, 62.70; H, 5.82; N, 21.47; S, 9.79%.

5-Amino-4-cyano-*N*-cyclohexyl-3-(4-fluorophenyl)-1*H*-pyrazole-1-carbothioamide (3b): brown crystals; IR (KBr, cm^{-1}) ν_{max}: 3352, 3299 (NH_2), 3151 (NH), 2972, 2854 (C-H, aliphatic), 2213 (CN), 1627 (C=N), 1534 (C=C), 1170 (C=S); ^{1}H-NMR (DMSO) δ (ppm): 11.49 (s, 1H, NH), 8.06 (s, 2H, NH_2), 7.96 (d, 2H, J = 8 *Hz*, Ar-H), 7.26 (d, 2H, J = 8 *Hz*, Ar-H), 4.46-1.12 (m, 11H, cyclohexyl-H); ^{13}C-NMR (DMSO) δ (ppm): 176.14 (C=S), 165.63, 160.95, 141.44, 131.22, 129.96, 116.66, 116.44 (CN), 116.05 (Ar-C), 51.87, 32.80, 25.63,

25.17 (cyclohexyl-C); MS (*m/z*, %): 343 (M^+, 81). Anal. Calcd for $C_{17}H_{18}FN_5S$ (343.42): C, 59.46; H, 5.28; N, 20.39; S, 9.34%. Found: C, 59.39; H, 5.18; N, 20.31; S, 9.28%.

5-Amino-3-(3-chlorophenyl)-4-cyano-*N*-cyclohexyl-1*H*-pyrazole-1-carbothioamide (3c): brown crystals; IR (KBr, cm^{-1}) ν_{max}: 3366, 3290 (NH_2), 3148 (NH), 2927, 2852 (C-H, aliphatic), 2209 (CN), 1625 (C=N), 1533 (C=C), 1156 (C=S); ^{1}H-NMR (DMSO) δ (ppm): 11.49 (s, 1H, NH), 8.70-7.43 (m, 4H, Ar-H), 8.01 (s, 2H, NH_2), 4.44-1.23 (m, 11H, cyclohexyl-H); ^{13}C-NMR (DMSO) δ (ppm): 176.00 (C=S), 161.14, 139.28, 136.41, 136.24, 134.19, 133.83, 128.34, 127.28, 114.77 (CN), 114.10 (Ar-C), 52.98, 31.41, 25.18, 24.87 (cyclohexyl-C); MS (*m/z*, %): 361 (M^++2, 27). Anal. Calcd for $C_{17}H_{18}ClN_5S$ (359.88): C, 56.74; H, 5.04; N, 19.46; S, 8.91%. Found: C, 56.67; H, 4.99; N, 19.39; S, 8.85%.

5-Amino-4-cyano-*N*-cyclohexyl-3-(*p*-tolyl)-1*H*-pyrazole-1-carbothioamide (3d): brown crystals; IR (KBr, cm^{-1}) ν_{max}: 3353, 3297 (NH_2), 3149 (NH), 2928, 2853 (C-H, aliphatic), 2210 (CN), 1622 (C=N), 1532 (C=C), 1176 (C=S); ^{1}H-NMR (DMSO) δ (ppm): 11.29 (s, 1H, NH), 7.99 (s, 2H, NH_2), 7.05 (d, 2H, *J* = 8 *Hz*, Ar-H), 6.97 (d, 2H, *J* =8 *Hz*, Ar-H), 4.43-1.21 (m, 11H, cyclohexyl-H), 2.40 (s, 3H, CH_3); ^{13}C-NMR (DMSO) δ (ppm): 173.84 (C=S), 168.73, 160.41, 130.12, 129.93, 128.00, 125.73, 116.04 (CN), 111.14 (Ar-C), 54.96, 32.51, 26.87, 26.41 (cyclohexyl-C), 21.87 (CH_3); MS (*m/z*, %): 339 (M^+, 48). Anal. Calcd for $C_{18}H_{21}N_5S$ (339.46): C, 63.69; H, 6.24; N, 20.63; S, 9.44%. Found: C, 63.60; H, 6.19; N, 20.57; S, 9.38%.

5-Amino-4-cyano-*N*-ethyl-3-phenyl-1*H*-pyrazole-1-carbothioamide (3e): brown crystals; IR (KBr, cm^{-1}) ν_{max}: 3364, 3310 (NH_2), 3188 (NH), 2973, 2868 (C-H, aliphatic), 2215 (CN), 1623 (C=N), 1542 (C=C), 1156 (C=S); ^{1}H-NMR (DMSO) δ (ppm): 11.43 (s, 1H, NH), 8.56-7.38 (m, 5H, Ar-H), 8.06 (s, 2H, NH_2), 3.51 (q, 2H, CH_2), 1.18 (t, 3H, CH_3); ^{13}C-NMR (DMSO) δ (ppm): 177.19 (C=S), 142.25, 134.70, 130.21, 129.10, 128.18, 127.68, 118.22 (CN), 111.83 (Ar-C), 39.76 (CH_2), 15.35 (CH_3); MS (*m/z*, %): 271 (M^+, 45). Anal. Calcd for $C_{13}H_{13}N_5S$ (271.34): C, 57.54; H, 4.83; N, 25.81; S, 11.82%. Found: C, 57.49; H, 4.77; N, 25.76; S, 11.76%.

5-Amino-4-cyano-*N*-ethyl-3-(4-fluorophenyl)-1*H*-pyrazole-1-carbothioamide (3f): brown crystals; IR (KBr, cm^{-1}) ν_{max}: 3363, 3306 (NH_2), 3193 (NH), 2975, 2875 (C-H, aliphatic), 2214 (CN), 1633 (C=N), 1547 (C=C), 1147 (C=S); ^{1}H-NMR (DMSO) δ (ppm): 11.42 (s, 1H, NH), 8.04 (s, 2H, NH_2), 7.97 (d, 2H, *J* =8 *Hz*, Ar-H), 7.28 (d, 2H, *J* = 8 *Hz*, Ar-H), 3.54 (q, 2H, CH_2), 1.17 (t, 3H, CH_3); ^{13}C-NMR (DMSO) δ (ppm): 177.17 (C=S), 164.65, 162.19, 141.07, 131.35, 129.90, 116.64, 116.24 (CN), 116.03 (Ar-C), 39.47 (CH_2), 15.34 (CH_3); MS (*m/z*, %): 289 (M^+, 54). Anal. Calcd for $C_{13}H_{12}FN_5S$ (289.33): C, 53.97; H, 4.18; N, 24.21; S, 11.08%. Found: C, 53.87; H, 4.11; N, 24.18, S, 11.00%.

5-Amino-3-(3-chlorophenyl)-4-cyano-*N*-ethyl-1*H*-pyrazole-1-carbothioamide (3g): brown crystals; IR (KBr, cm^{-1}) ν_{max}: 3346, 3304 (NH_2), 3185 (NH), 2994, 2885 (C-H, aliphatic), 2211 (CN), 1634 (C=N), 1567 (C=C), 1141 (C=S); ^{1}H-NMR (DMSO) δ (ppm): 11.51 (s, 1H, NH), 8.52-7.51 (m, 4H, Ar-H), 8.03 (s, 2H, NH_2), 3.50 (q, 2H, CH_2), 1.18 (t, 3H, CH_3); ^{13}C-NMR (DMSO) δ (ppm): 175.18 (C=S), 166.65, 160.40, 134.18, 134.14, 129.22, 129.13, 128.20, 125.11, 115.69 (CN), 112.81 (Ar-C), 39.06 (CH_2), 16.34 (CH_3); MS (*m/z*, %): 307 (M^++2, 21). Anal. Calcd for $C_{13}H_{12}ClN_5S$ (305.78): C, 51.06; H, 3.96; N, 22.90; S, 10.48%. Found: C, 51.00; H, 3.89; N, 22.83; S, 10.39%.

5-Amino-4-cyano-*N*-ethyl-3-(*p*-tolyl)-1*H*-pyrazole-1-carbothioamide (3h): brown crystals; IR (KBr, cm^{-1}) ν_{max}: 3354, 3294 (NH_2), 3153 (NH), 2991, 2936 (C-H, aliphatic), 2212 (CN), 1631 (C=N), 1548 (C=C), 1159 (C=S); ^{1}H-NMR (DMSO) δ (ppm): 11.31 (s, 1H, NH),

8.00 (s, 2H, NH_2), 7.76 (d, 2H, *J* = 8 *Hz*, Ar-H), 6.99 (d, 2H, *J* = 8 *Hz*, Ar-H), 3.63 (q, 2H, CH_2), 2.51 (s, 3H, CH_3), 1.17 (t, 3H, CH_3); ^{13}C-NMR (DMSO) δ (ppm): 177.68 (C=S), 166.15, 159.08, 131.70, 129.14, 128.80, 125.02, 116.89 (CN), 113.01 (Ar-C), 38.96 (CH_2), 21.20 (CH_3), 15.34 (CH_3); MS (*m/z*, %): 285 (M^+, 59). Anal. Calcd for $C_{14}H_{15}N_5S$ (285.37): C, 58.93; H, 5.30; N, 24.54; S, 11.23%. Found: C, 58.85; H, 5.22; N, 24.51; S, 11.17%.

5-Amino-4-cyano-*N*-methyl-3-phenyl-1*H*-pyrazole-1-carbothioamide (3i): yellow crystals; IR (KBr, cm^{-1}) ν_{max}: 3336, 3274 (NH_2), 3151 (NH), 2991 (C-H, aliphatic), 2211 (CN), 1620 (C=N), 1549 (C=C), 1177 (C=S); ^{1}H-NMR (DMSO) δ (ppm): 11.49 (s, 1H, NH), 8.52-7.52 (m, 5H, Ar-H), 8.05 (s, 2H, NH_2), 2.76 (s, 3H, CH_3); ^{13}C-NMR (DMSO) δ (ppm): 178.23 (C=S), 142.14, 134.75, 130.20, 129.11, 128.94, 127.65, 115.59 (CN), 101.91 (Ar-C), 31.31 (CH_3); MS (*m/z*, %): 257 (M^+, 33). Anal. Calcd for $C_{12}H_{11}N_5S$ (257.32): C, 56.01; H, 4.31; N, 27.22; S, 12.46%. Found: C, 56.08; H, 4.27; N, 27.12; S, 12.40%.

5-Amino-4-cyano-3-(4-fluorophenyl)-*N*-methyl-1*H*-pyrazole-1-carbothioamide (3j): brown crystals; IR (KBr, cm^{-1}) ν_{max}: 3288, 3235 (NH_2), 3150 (NH), 2927 (C-H, aliphatic), 2210 (CN), 1631 (C=N), 1559 (C=C), 1171 (C=S); ^{1}H-NMR (DMSO) δ (ppm): 11.51 (s, 1H, NH), 8.04 (s, 2H, NH_2), 7.96 (d, 2H, *J* = 8 *Hz*, Ar-H), 7.29 (d, 2H, *J* = 8 *Hz*, Ar-H), 2.89 (s, 3H, CH_3); ^{13}C-NMR (DMSO) δ (ppm): 178.19 (C=S), 165.63, 160.96, 140.96, 130.88, 127.32, 116.67, 115.98 (CN), 115.76 (Ar-C), 31.29 (CH_3); MS (*m/z*, %): 275 (M^+, 61). Anal. Calcd for $C_{12}H_{10}FN_5S$ (275.31): C, 52.35; H, 3.66; N, 25.44; S, 11.65%. Found: C, 52.30; H, 3.58; N, 25.39; S, 11.58%.

5-Amino-3-(3-chlorophenyl)-4-cyano-*N*-methyl-1*H*-pyrazole-1-carbothioamide (3k): yellow crystals; IR (KBr, cm^{-1}) ν_{max}: 3344, 3289 (NH_2), 3146 (NH), 2929 (C-H, aliphatic), 2204 (CN), 1624 (C=N), 1563 (C=C), 1164 (C=S); ^{1}H-NMR (DMSO) δ (ppm): 11.53 (s, 1H, NH), 8.43-7.44 (m, 4H, Ar-H), 8.04 (s, 2H, NH_2), 2.80 (s, 3H, CH_3); ^{13}C-NMR (DMSO) δ (ppm): 178.28 (C=S), 161.13, 140.45, 136.54, 136.25, 134.22, 134.19, 131.66, 129.79, 124.77 (CN), 124.12 (Ar-C), 31.34 (CH_3); MS (*m/z*, %): 293 (M^++2, 16). Anal. Calcd for $C_{12}H_{10}ClN_5S$ (291.76): C, 49.40; H, 3.45; N, 24.00; S, 10.99%. Found: C, 49.32; H, 3.38; N, 23.94; S, 10.90%.

5-Amino-4-cyano-*N*-methyl-3-(*p*-tolyl)-1*H*-pyrazole-1-carbothioamide (3l): brown crystals; IR (KBr, cm^{-1}) ν_{max}: 3409, 3320 (NH_2), 3158 (NH), 2968 (C-H, aliphatic), 2208 (CN), 1632 (C=N), 1552 (C=C), 1167 (C=S); ^{1}H-NMR (DMSO) δ (ppm): 11.37 (s, 1H, NH), 8.00 (s, 2H, NH_2), 7.76 (d, 2H, *J* = 8 *Hz*, Ar-H), 6.99 (d, 2H, *J* = 8 *Hz*, Ar-H), 3.01 (s, 3H, CH_3), 2.51 (s, 3H, CH_3); ^{13}C-NMR (DMSO) δ (ppm): 176.98 (C=S), 163.93, 148.33, 131.18, 129.32, 128.02, 125.55, 114.08 (CN), 109.19 (Ar-C), 33.34 (CH_3), 21.54 (CH_3); MS (*m/z*, %): 271 (M^+, 37). Anal. Calcd for $C_{13}H_{13}N_5S$ (271.34): C, 57.54; H, 4.83; N, 25.81; S, 11.82%. Found: C, 57.49; H, 4.75; N, 25.75; S, 11.77%.

5-Amino-4-cyano-*N*-(4-methoxybenzyl)-3-phenyl-1*H*-pyrazole-1-carbothioamide (3m): brown crystals; IR (KBr, cm^{-1}) ν_{max}: 3344, 3306 (NH_2), 3157 (NH), 2985 (C-H, aliphatic), 2211 (CN), 1620 (C=N), 1583 (C=C), 1180 (C=S); ^{1}H-NMR (DMSO) δ (ppm): 11.78 (s, 1H, NH), 8.16 (s, 2H, NH_2), 7.92-6.93 (m, 9H Ar-H), 3.40 (s, 3H, OCH_3), 2.94 (s, 2H, CH_2); ^{13}C-NMR (DMSO) δ (ppm): 176.86 (C=S), 162.03, 157.44, 143.13, 134.53, 132.40, 131.90, 130.46, 129.43, 128.05, 125.61, 113.73 (CN), 111.81 (Ar-C), 55.70 (OCH_3), 40.28 (CH_2); MS (*m/z*, %): 363 (M^+, 43). Anal. Calcd for $C_{19}H_{17}N_5OS$ (363.44): C, 62.79; H, 4.71; N, 19.27; S, 8.82%. Found: C, 62.70; H, 4.66; N, 19.19; S, 8.75%.

5-Amino-4-cyano-3-(4-fluorophenyl)-*N*-(4-methoxybenzyl)-1*H*-pyrazole-1-carbothioamide (3n): brown crystals; IR (KBr, cm^{-1}) ν_{max}: 3354, 3307 (NH_2), 3156 (NH), 2924

(C-H, aliphatic), 2210 (CN), 1631 (C=N), 1580 (C=C), 1176 (C=S); ^{1}H-NMR (DMSO) δ (ppm): 11.48 (s, 1H, NH), 8.01 (s, 2H, NH_2), 7.50 (d, 2H, *J* = 8 *Hz*, Ar-H), 7.38 (d, 2H, *J* = 8 *Hz*, Ar-H), 7.33-6.32 (m, 4H, Ar-H), 3.34 (s, 3H, OCH_3), 2.89 (s, 2H, CH_2); ^{13}C-NMR (DMSO) δ (ppm): 179.91 (C=S), 160.67, 158.64, 148.66, 138.03, 132.60, 130.76, 130.06, 126.03, 116.95, 116.01 (CN), 114.83, 114.11 (Ar-C), 52.93 (OCH_3), 39.50 (CH_2); MS (*m/z*, %): 381 (M^+, 29). Anal. Calcd for $C_{19}H_{16}FN_5OS$ (381.43): C, 59.83; H, 4.23; N, 18.36; S, 8.41%. Found: C, 59.75; H, 4.17; N, 18.30; S, 8.35%.

2.1. Molecular docking part.

The standard docking protocol using MOE 2015.10 software was used to study the interaction between the designed compounds 3a-n and TPP, the binding site of COX-2 enzyme (pdb code:3LN1), compared with celecoxib as a reference drug.

3. Results and Discussion

3.1. Chemistry.

Recently, we have established the interaction between $ZnCl_2$ nano-flakes and nanocrystalline hydroxyapatite (HAp) using both Fourier-transform infrared spectroscopy (FTIR) and X-ray diffraction (XRD). FTIR spectral data revealed a physical interaction between them without any evidence of chemical interaction, while XRD revealed sharp peaks attributed to HAp in their position without any indication for the presence of secondary phases. The idea of $ZnCl_2$ nano-flakes adsorbed on the surface of the nano-HAp was also supported by scanning electron microscopy (SEM) and energy dispersive X-ray (EDX) [22]. All presented data show a homogeneous distribution of the catalyst.

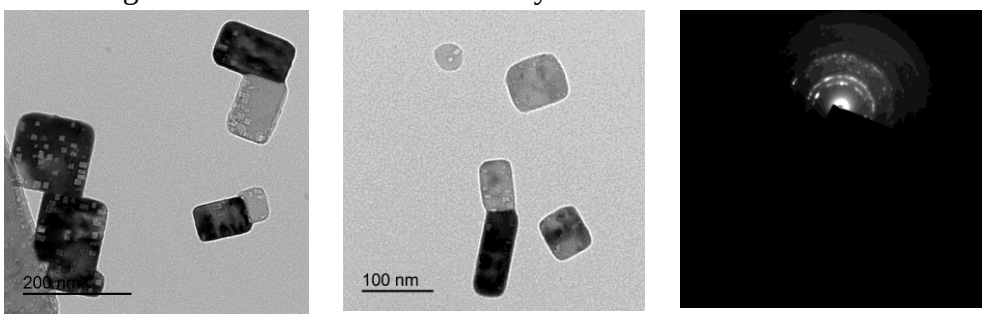

Figure 2. TEM of hydroxyapatite loaded with $ZnCl_2$

In the present study, additional support was included, in particular, the transmission electron microscopy (TEM) supported by electron diffraction, which shows a variation of the geometrical shape of HAp (nano-rods) with $ZnCl_2$, adsorbed on the surface, to give a flake-like structure (Figure 2). The target compounds, 5-amino-3-aryl-4-cyano-*N*-cyclohexyl-1*H*-pyrazole-1-carbothioamide derivatives 3a-d, were synthesized via a one-pot multicomponent reaction of hydrazine hydrate, arylidene malononitrile, cyclohexyl isothiocyanate, and HAp/$ZnCl_2$ as a catalyst. The reaction conditions were optimized, and excellent results were obtained without solvent at 60-70°C, with high yields of the products (80-90%) in shorter reaction times (30-40 min). The structure of products 3a-d was confirmed by elemental analyses and spectral studies. As exemplified for product 3a as follows: the IR spectrum showed absorption bands due to NH_2, NH, CN, and C=S groups at 3344-3290, 3150, 2211, and 1159 cm^{-1}, respectively. In the ^{1}H NMR spectrum, we observed aromatic signals at δ 7.95-7.35 ppm and two broad singlet signals at δ 11.45 and 8.08 ppm due to NH and NH_2 protons (D_2O

exchangeable), respectively. Besides, the cyclohexyl protons presented a set of signals centered at δ 4.44-1.23 ppm. The cyano and C=S groups appeared at δ 114.00 and 173.85 ppm, respectively, in the ^{13}C NMR spectrum. Finally, the mass spectrum supported the structural assignment *m/z* 325 $[M]^+$. Encouraged by the above results and under the same optimized conditions, we have successfully applied this new methodology to synthesize new 1*H*-pyrazole-1-carbothioamide derivatives 3e-n using various substituted isothiocyanate and arylidene malononitrile. The reaction proceeds very smoothly and gives yields up to 95% in short reaction times without the formation of any byproducts, as monitored by TLC (Scheme 1 and Table 1).

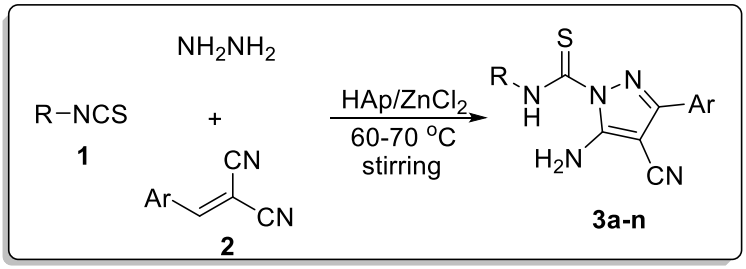

Scheme 1. Synthesis of 1*H*-pyrazole-1-carbothioamide derivatives 3a-n.

A plausible mechanism for the formation of 1*H*-pyrazole-1-carbothioamide derivatives 3a-n is proposed in Scheme 2. Initially, the nucleophilic attack of hydrazine hydrate to isothiocyanates gives the thiosemicarbazides I. Then, the nucleophilic addition of the amino group in I to the activated double bond in arylidene malononitrile II results in acyclic intermediates III, which subsequently undergo intramolecular cyclization, tautomerization and aerial oxidation to afford the target compounds.

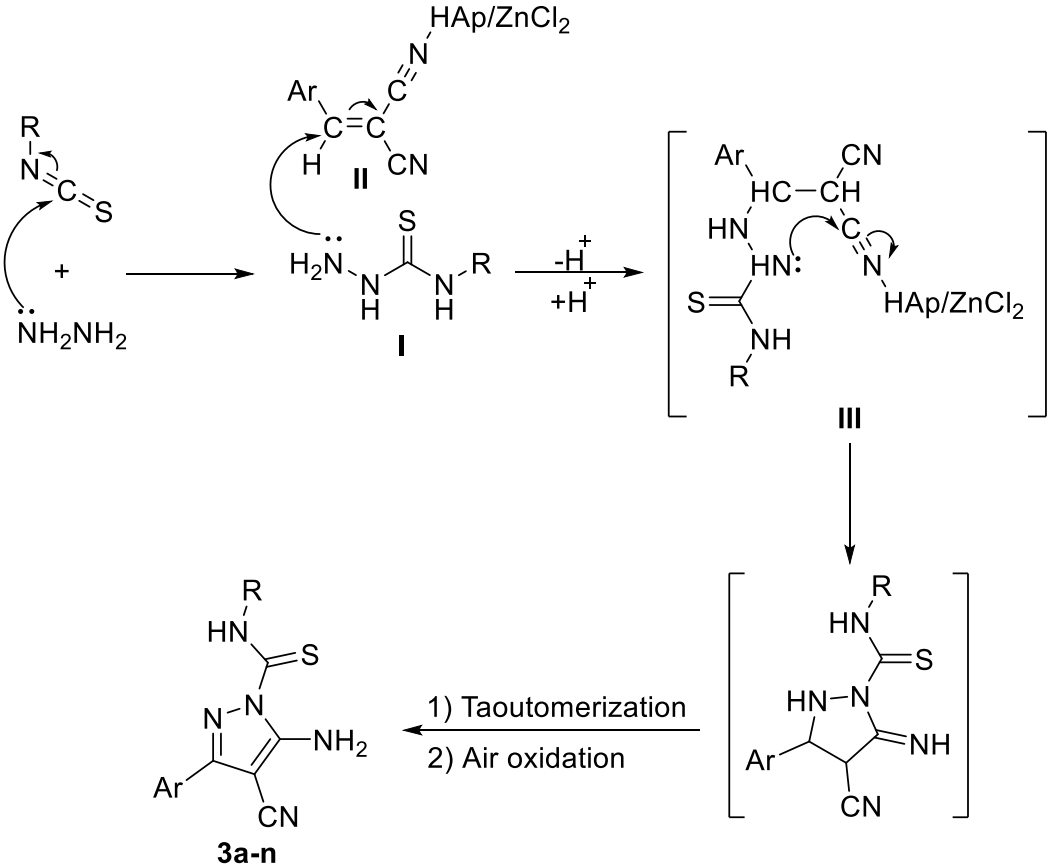

Scheme 2. A proposed reaction mechanism for the formation of 1*H*-pyrazole-1-carbothioamide derivatives 3a-n.

Table 1. Synthesis of 1*H*-pyrazole-1-carbothioamide derivatives 3a-n using HAp/$ZnCl_2$ nano-flakes at 60-70°C without solvent.

Entry	Product	Ar	R	Time (min)	Mp (°C)	Yield (%)
1	**3a**	C_6H_5	C_6H_{11}	40	138	85
2	**3b**	4-FC_6H_4	C_6H_{11}	30	108	90
3	**3c**	3-ClC_6H_4	C_6H_{11}	35	120	88
4	**3d**	4-$CH_3C_6H_4$	C_6H_{11}	40	126	80
5	**3e**	C_6H_5	C_2H_5	30	128	82
6	**3f**	4-FC_6H_4	C_2H_5	40	175	90
7	**3g**	3-ClC_6H_4	C_2H_5	50	100	92
8	**3h**	4- $CH_3C_6H_4$	C_2H_5	35	150	80
9	**3i**	C_6H_5	CH_3	30	130	80
10	**3j**	4-FC_6H_4	CH_3	40	140	95
11	**3k**	3-ClC_6H_4	CH_3	35	118	88
12	**3l**	4- $CH_3C_6H_4$	CH_3	50	158	76
13	**3m**	C_6H_5	4-$(CH_3O)C_6H_4CH_2$	50	150	78
14	**3n**	4-FC_6H_4	4-$(CH_3O)C_6H_4CH_2$	40	148	79

3.2. Molecular docking study.

The binding site of the COX-2 enzyme has two additional pockets, which are absent in the COX-1 enzyme [27]. The two additional binding pockets are believed to be responsible for the selectivity of COX-2 inhibitors. The molecular docking validation [28] explains that compounds 3d, 3e, 3h, and 3n show the highest selectivity when dock into the binding site of the COX-2 enzyme compared with celecoxib as a reference drug. Figure 3 explains the docking validation by calculating the energy score (E-score), which reflects the ability of drug-receptor interaction and calculating the root mean square deviation (RMSD), reflecting the stereo suitability of drug with the selective receptor pocket, low values refer to better results. The active site analysis of the COX-2 protein receptor was performed from a database similar to amino acid residues using the MOE2015.10 software, Leu338, Gln178, Gly512, Ala502, Ala513, Leu370, Ser516, Tyr371, Vel102, Phe367, Trp373, Arg106, Leu345, Leu517, Gly340, Met99, Ile503, Tir341, Met503, Val509, Arg499, Phe504, Val335, His75, and Ser339.

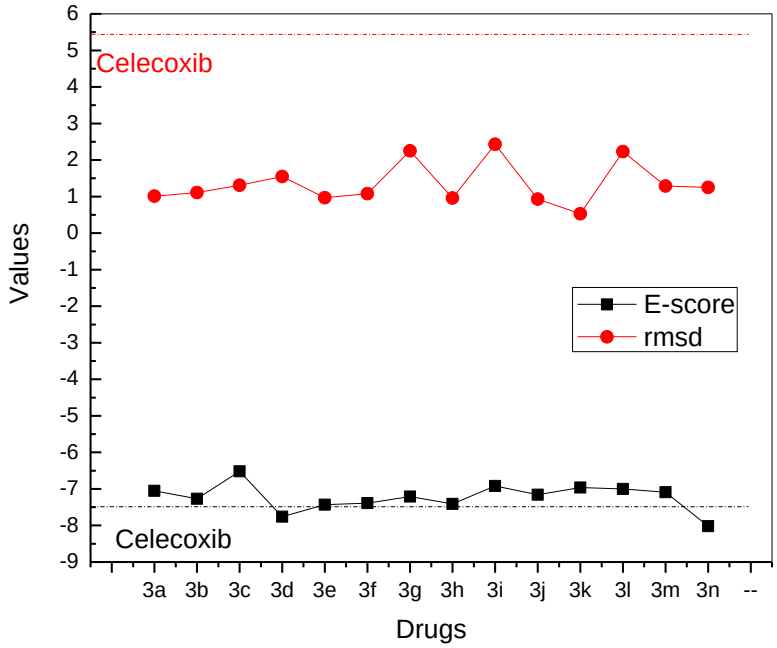

Figure 3. E-score and rmsd values for the prepared compounds compared with celecoxib.

The 2D pocket in the COX-2 receptor complex with celecoxib explains that the interaction between them is potent with good E-score values through the formation of hydrogen

bonds, but the "rmsd" value is very high, and this decreases the suitability of this drug towards COX-2. The four prepared compounds (3d, 3e, 3h, and 3n) exhibit more potent interaction with the COX-2 receptor than the reference drug with very good E-score and low "rmsd" values, which reflects the ability of our prepared compounds to interact with the active site of the COX-2 receptor. The computational docking study was explained by 2D and 3D interaction for the four prepared compounds, as exemplified for product 3h compared with the reference drug (Figures 4 and 5).

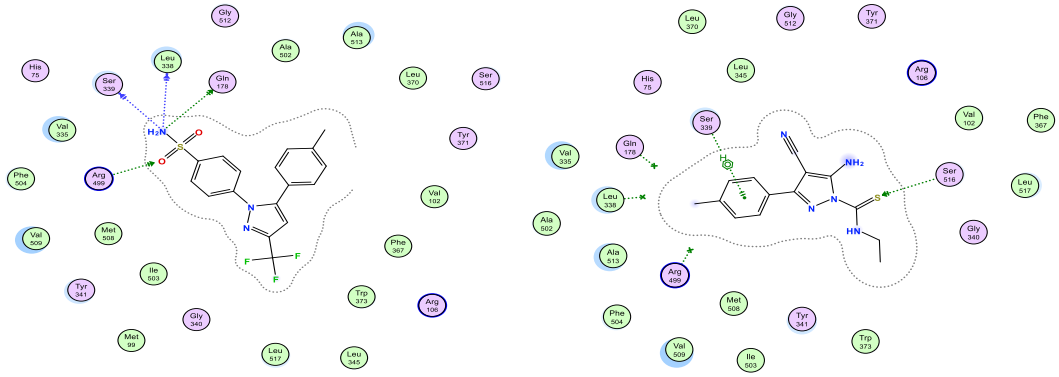

Celecoxib compound **3h**

Figure 4. The 2D interaction of the COX-2 receptor with celecoxib and compound 3h.

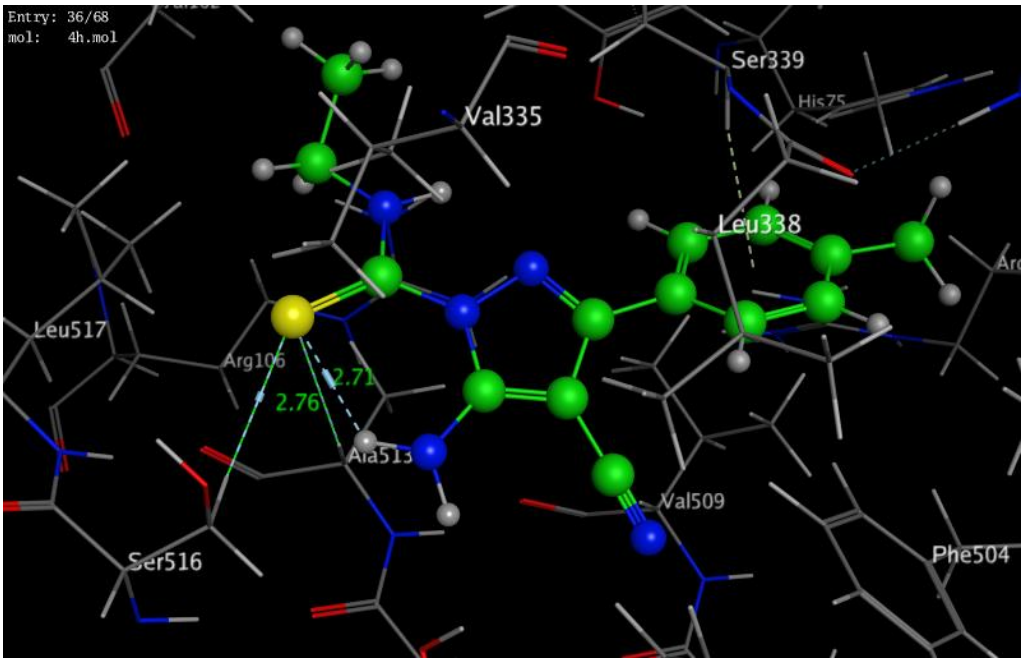

Figure 5. The 3D interaction of the COX-2 receptor with compound 3h with the two-hydrogen bond length.

The concept of pharmacophore has been widely applied in the rational design of new drugs. A pharmacophore is known as a set of steric and electronic characteristics needful to ensure optimal supramolecular interactions with a particular biological target and prevent or trigger its biological activity [29]. The most potent compounds (3d, 3e, 3h, and 3n) were selected and examined to build a pharmacophore for potential COX-2 inhibitors and showed promising results. As exemplified for product 3n (Figure 6), generated a pharmacophore with H-bond acceptor (Acc, Acc2), H-bond donor (Don), aromatic (Aro), and hydrophobic (hyd) centers.

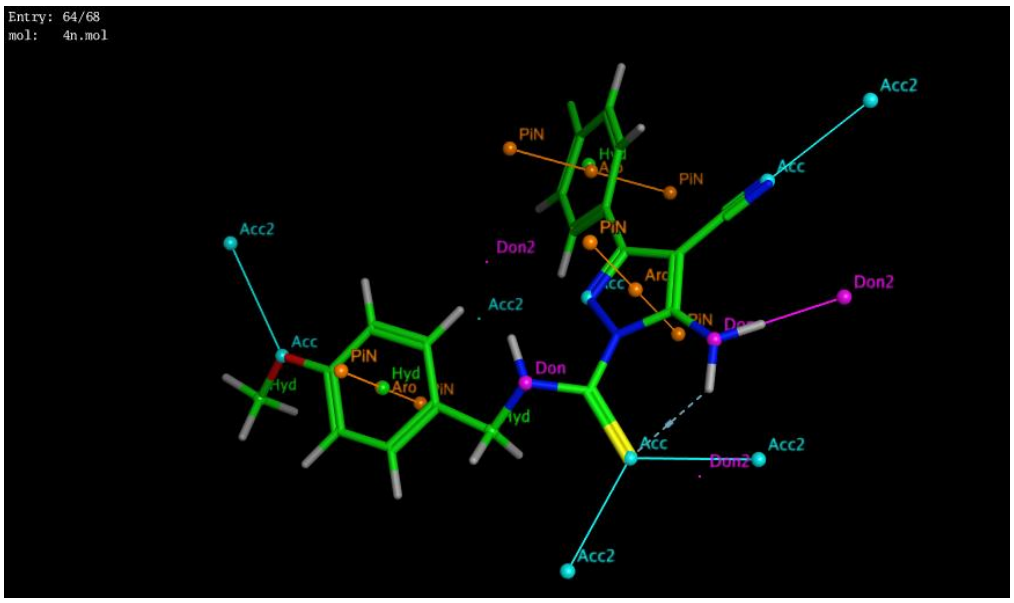

Figure 6. 3D pharmacophore structure of 3n simulated to the active site of COX-2.

4. Conclusions

We have described an efficient and straightforward catalytic synthesis of new 1*H*-pyrazole-1-carbothioamide derivatives through a one-pot reaction of hydrazine hydrate, arylidene malononitrile, and isothiocyanates in the presence of HAp/$ZnCl_2$ nano-flakes at 60-70 ºC. The whole reaction process has the advantages of mild condition, simple operation, high yield, short reaction time, and at the same time, HAp/$ZnCl_2$ nano-flakes demonstrated an excellent tolerance in the synthesis of target compounds. It is suitable for the industrial production of high efficient green synthesis technology. The molecular docking study as COX-2 inhibitors explained that compounds 3d, 3e, 3h, and 3n show promising results compared with celecoxib as a reference drug.

Funding

This research received no external funding.

Acknowledgments

We present our sincere thanks and gratitude to the National Research Centre and Faculty of Science, Mansoura University, for continuous support.

Conflicts of Interest

The authors declare no conflict of interest.

References

1. Serhan, C.N. Treating inflammation and infection in the 21st century: new hints from decoding resolution mediators and mechanisms. *The FASEB Journal* **2017**, *31*, 1273-1288, https://doi.org/10.1096/fj.201601222R.
2. Hassan, G.S.; Abdel Rahman, D.E.; Abdelmajeed, E.A.; Refaey, R.H.; Alaraby Salem, M.; Nissan, Y.M. New pyrazole derivatives: Synthesis, anti-inflammatory activity, cycloxygenase inhibition assay and evaluation of mPGES. *Eur. J. Med. Chem.* **2019**, *171*, 332-342, https://doi.org/10.1016/j.ejmech.2019.03.052.

3. Poetker, D.M.; Reh, D.D. A Comprehensive Review of the Adverse Effects of Systemic Corticosteroids. *Otolaryngol. Clin. North Am.* **2010**, *43*, 753-768, https://doi.org/10.1016/j.otc.2010.04.003.
4. Day, R.O.; Graham, G.G. Non-steroidal anti-inflammatory drugs (NSAIDs). *BMJ* **2013**, *346*, f3195, https://doi.org/10.1136/bmj.f3195.
5. Harirforoosh, S.; Asghar, W.; Jamali, F. Adverse Effects of Nonsteroidal Antiinflammatory Drugs: An Update of Gastrointestinal, Cardiovascular and Renal Complications. *Journal of Pharmacy & Pharmaceutical Sciences* **2014**, *16*, 821-847, https://doi.org/10.18433/J3VW2F.
6. Rao, P.P.N.; Kabir, S.N.; Mohamed, T. Nonsteroidal Anti-Inflammatory Drugs (NSAIDs): Progress in Small Molecule Drug Development. *Pharmaceuticals* **2010**, *3*, https://doi.org/10.3390/ph3051530.
7. Rouzer, C.A.; Marnett, L.J. Cyclooxygenases: structural and functional insights. *J. Lipid Res.* **2009**, *50*, S29-S34, https://doi.org/10.1194/jlr.R800042-JLR200.
8. Seibert, K.; Masferrer, J.L. Role of inducible cyclooxygenase (COX-2) in inflammation. *Receptor* **1994**, *4*, 17-23.
9. Jose, M.-G.; Lina, B. Mechanisms Underlying the Cardiovascular Effects of COX-Inhibition: Benefits and Risks. *Curr. Pharm. Des.* **2007**, *13*, 2215-2227, https://doi.org/10.2174/138161207781368774.
10. Karrouchi, K.; Radi, S.; Ramli, Y.; Taoufik, J.; Mabkhot, Y.N.; Al-aizari, F.A.; Ansar, M.h. Synthesis and Pharmacological Activities of Pyrazole Derivatives: A Review. *Molecules* **2018**, *23*, https://doi.org/10.3390/molecules23010134.
11. Thi, T.H.N.; Thi, Y.T.; Nguyen, L.A.; Vo, N.B.; Ngo, Q.A. Design, Synthesis and Biological Activities of New Pyrazole Derivatives Possessing Both Coxib and Combretastatins Pharmacophores. *Chem. Biodivers.* **2019**, *16*, e1900108, https://doi.org/10.1002/cbdv.201900108.
12. Ali, S.A.; Awad, S.M.; Said, A.M.; Mahgoub, S.; Taha, H.; Ahmed, N.M. Design, synthesis, molecular modelling and biological evaluation of novel 3-(2-naphthyl)-1-phenyl-1H-pyrazole derivatives as potent antioxidants and 15-Lipoxygenase inhibitors. *J. Enzyme Inhib. Med. Chem.* **2020**, *35*, 847-863, https://doi.org/10.1080/14756366.2020.1742116.
13. Assali, M.; Abualhasan, M.; Sawaftah, H.; Hawash, M.; Mousa, A. Synthesis, Biological Activity, and Molecular Modeling Studies of Pyrazole and Triazole Derivatives as Selective COX-2 Inhibitors. *Journal of Chemistry* **2020**, *2020*, 6393428, https://doi.org/10.1155/2020/6393428.
14. Macarini, A.F.; Sobrinho, T.U.C.; Rizzi, G.W.; Corrêa, R. Pyrazole–chalcone derivatives as selective COX-2 inhibitors: design, virtual screening, and in vitro analysis. *Med. Chem. Res.* **2019**, *28*, 1235-1245, https://doi.org/10.1007/s00044-019-02368-8.
15. Murahari, M.; Mahajan, V.; Neeladri, S.; Kumar, M.S.; Mayur, Y.C. Ligand based design and synthesis of pyrazole based derivatives as selective COX-2 inhibitors. *Bioorg. Chem.* **2019**, *86*, 583-597, https://doi.org/10.1016/j.bioorg.2019.02.031.
16. Faisal, M.; Saeed, A.; Hussain, S.; Dar, P.; Larik, F.A. Recent developments in synthetic chemistry and biological activities of pyrazole derivatives. *Journal of Chemical Sciences* **2019**, *131*, 70, https://doi.org/10.1007/s12039-019-1646-1.
17. Nozari, M.; Addison, A.W.; Reeves, G.T.; Zeller, M.; Jasinski, J.P.; Kaur, M.; Gilbert, J.G.; Hamilton, C.R.; Popovitch, J.M.; Wolf, L.M.; Crist, L.E.; Bastida, N. New Pyrazole- and Benzimidazole-derived Ligand Systems. *J. Heterocycl. Chem.* **2018**, *55*, 1291-1307, https://doi.org/10.1002/jhet.3155.
18. Kelada, M.; Walsh, J.M.D.; Devine, R.W.; McArdle, P.; Stephens, J.C. Synthesis of pyrazolopyrimidinones using a “one-pot” approach under microwave irradiation. *Beilstein J. Org. Chem.* **2018**, *14*, 1222-1228, https://doi.org/10.3762/bjoc.14.104.
19. Piltan, M. Preparation of 1H-pyrazolo[1,2-b]phthalazine-5,10-diones using ZrO2 nanoparticles as a catalyst under solvent-free conditions. *Heterocycl. Commun.* **2017**, *23*, 401-403, https://doi.org/10.1515/hc-2017-0142.
20. Zolfigol, M.A.; Afsharnadery, F.; Baghery, S.; Salehzadeh, S.; Maleki, F. Catalytic applications of {[HMIM]C(NO2)3}: as a nano ionic liquid for the synthesis of pyrazole derivatives under green conditions and a mechanistic investigation with a new approach. *RSC Advances* **2015**, *5*, 75555-75568, https://doi.org/10.1039/C5RA16289K.
21. Maddila, S.; Rana, S.; Pagadala, R.; Kankala, S.; Maddila, S.; Jonnalagadda, S.B. Synthesis of pyrazole-4-carbonitrile derivatives in aqueous media with CuO/ZrO2 as recyclable catalyst. *Catal. Commun.* **2015**, *61*, 26-30, https://doi.org/10.1016/j.catcom.2014.12.005.

22. Khatab, T.K.; Abdelghany, A.M.; Kandil, E.M.; Elsefy, D.E.; El-Mekabaty, A. Hydroxyapatite/ZnCl2 nano-flakes: an efficient catalyst for the synthesis of 2-arylbenzothiazoles with molecular docking and anti-oxidant evaluation. *Biointerface Res Appl Chem* **2020**, *10*, 5182-5187, https://doi.org/10.33263/BRIAC102.182187.
23. Abdelghany, A.M.; Menazea, A.A.; Abd-El-Maksoud, M.A.; Khatab, T.K. Pulsed laser ablated zeolite nanoparticles: A novel nano-catalyst for the synthesis of 1,8-dioxo-octahydroxanthene and N-aryl-1,8-dioxodecahydroacridine with molecular docking validation. *Appl. Organomet. Chem.* **2020**, *34*, e5250, https://doi.org/10.1002/aoc.5250.
24. Sroor, F.M.; Khatab, T.K.; Basyouni, W.M.; El-Bayouki, K.A.M. Synthesis and molecular docking studies of some new thiosemicarbazone derivatives as HCV polymeraseinhibitors. *Synth. Commun.* **2019**, *49*, 1444-1456, https://doi.org/10.1080/00397911.2019.1605443.
25. Khatab, T.K.; Abdelghany, A.M.; Soliman, H.A. V2O5 based quadruple nano-perovskite as a new catalyst for the synthesis of bis and tetrakis heterocyclic compounds. *Appl. Organomet. Chem.* **2019**, *33*, e4783, https://doi.org/10.1002/aoc.4783.
26. Khatab, T.K.; Abdelghany, A.M.; Shaker, N.; Osama, Y.; Kandil, E.M. Evaluation of the Optical and Structural Properties of Constructed Bis-indole Derivatives Using (Sm2O3/SiO2) Catalyst. *Silicon* **2018**, *10*, 2173-2179, https://doi.org/10.1007/s12633-017-9747-2.
27. Meade, E.A.; Smith, W.L.; Dewitt, D.L. Differential inhibition of prostaglandin endoperoxide synthase (cyclooxygenase) isozymes by aspirin and other non-steroidal anti-inflammatory drugs. *J. Biol. Chem.* **1993**, *268*, 6610-6614, https://doi.org/10.1016/S0021-9258(18)53294-4.
28. Wang, J.L.; Limburg, D.; Graneto, M.J.; Springer, J.; Hamper, J.R.B.; Liao, S.; Pawlitz, J.L.; Kurumbail, R.G.; Maziasz, T.; Talley, J.J.; Kiefer, J.R.; Carter, J. The novel benzopyran class of selective cyclooxygenase-2 inhibitors. Part 2: The second clinical candidate having a shorter and favorable human half-life. *Bioorg. Med. Chem. Lett.* **2010**, *20*, 7159-7163, https://doi.org/10.1016/j.bmcl.2010.07.054.
29. Daisy, P.; Singh, S.K.; Vijayalakshmi, P.; Selvaraj, C.; Rajalakshmi, M.; Suveena, S. A database for the predicted pharmacophoric features of medicinal compounds. *Bioinformation* **2011**, *6*, 167–168, doi: 10.6026/97320630006167.